View metadata, citation and similar papers at core.ac.uk
brought to you by CORE
provided by Repository@USM

DEVELOPMENT OF MICROWAVE BANDPASS FILTER USING DEFECTED GROUND STRUCTURE IN COMPARISON WITH MULTILAYER AND DIELECTRIC RESONATOR FILTERS

AHMAD ASARI SULAIMAN

UNIVERSITI SAINS MALAYSIA
2012

DEVELOPMENT OF MICROWAVE BANDPASS FILTER USING DEFECTED GROUND STRUCTURE IN COMPARISON WITH MULTILAYER AND DIELECTRIC RESONATOR FILTERS

by

AHMAD ASARI SULAIMAN

Thesis submitted in fulfillment of the requirements
for the degree of
Doctor of Philosophy
in Electrical and Electronics Engineering
UNIVERSITI SAINS MALAYSIA

JANUARY 2012

Acknowledgements

I would like to thank my supervisor Associate Professor Dr. Mohd Fadzil Ain from the School of Electrical & Electronics Engineering for his patience, constructive criticism and directions at every junction wherever I encounter challenges. He was constantly encouraging me at a stage when I almost give up. I am also indebted to my co-supervisor in person of Professor Dr. Zainal Arifin Ahmad from the School of Materials & Mineral Resources Engineering for his thoroughness and diligence. In fact, he is a perfectionist. This work would not have been possible without their guidance and inputs. I also want to thank the Dean of the school of Electrical and Electronics Engineering Professor Dr. Zaid Abdullah and the Deputy Dean of Research and Postgraduate, Associate Professor Dr. Kamal Zuhairi Zamli for their support and encouragement through the completion of this programme.

My deepest and special thanks go to the Universiti Teknologi MARA, Universiti Sains Malaysia and the Ministry Of Science, Technology and Innovation (MOSTI) for the financial support. I would also like to thank all my colleagues and staff at both Schools of Electrical & Electronics Engineering and Materials & Mineral Resources Engineering who have assisted me in numerous ways.

Finally, I specifically want to thank my wife Junita Jusoh, my children: Arfan, Afif, Auni and my parents for their endurance, support and encouragement during course of this study.

Table of Contents

Acknowledgements ii

Table of Contents iii

List of Figures viii

List of Tables xiv

List of Abbreviations xv

List of Symbols xvii

ABSTRAK xx

ABSTRACT xxii

1.0 INTRODUCTION 1

1.1 Background and Motivation 1

1.2 Problem Statement 3

1.3 Objectives 5

1.4 Scope of Works 6

1.5 Thesis Organization 8

2.0 LITERATURE REVIEW 10

2.1 Introduction 10

2.2 Review on the Concept of Aperture Slot 11

2.3 Basic Properties of DGS 12

2.4 Electromagnetic Band Gap (EBG) 13

2.5 Uniplanar-Compact EBG Structures 15

2.6 Multilayer EBG Structures 18

2.7 Defected Ground Structure (DGS) 19

2.8 Perforation in Transmission Lines 20

2.9 Problems of Conventional Microstrip EBG Structures 23

2.10 Microstrip DGS Structures 26

2.10.1 Corrugated Slots 28

2.10.2 Folded Slots with T-Shaped Metal-Loading 29

2.10.3 Transmission Line Model of the Folded Slot Resonators with the T-Shaped Metal-Loading 31

2.10.4 RLC Lumped-Element Circuit Model 35

2.11 Interdigital, Parallel-Coupled and Folded Slot Bandpass Filters 37

2.12 Various Types of Dielectric Resonator Filters 40

2.12.1 Transverse Electric (TE) Mode DR Filter for Cellular Base-Station 40

2.12.2 Transverse Magnetic Mode DR Filter 41

2.12.3 Dual-Mode DR Filter 42

2.12.4 Quadruple-Mode DR Filter 43

2.13 Basic type of Filters 47

2.14 Return and Insertion Losses 50

2.15 Poles and Zeros 53

2.16 Improvement of insertion loss by the DGS 53

2.17 Wideband Bandpass Filters 54

2.18 Transmission Line Filters 54

2.19 Quarter-Wave Transmission-Line Filters 55

2.20 Parallel-Coupled Filters 56

2.21 Methods and Tools to Analyze DGS and EBG Structures 58

2.22 Detail Electromagnetic (EM) Analysis of DGS and EBG 59

2.23 Dielectric Resonator Filters 64

2.23.1 Dielectric Resonators (DRs) 65

2.23.2 Dielectric Constant, ε 66

2.23.3 Quality Factor, Q 66

2.23.4 Characteristic of Dielectric Resonator 68

2.23.5 The Cylindrical Shape of Dielectric Resonator 69

2.24 Coupling to DRs 69

2.24.1 Fields within Cylindrical DRs 71
2.24.2 Microstrip Line Coupling 72
2.24.3 Multiple DRs 73
2.25 Air Gaps 74
2.26 Design of Feed Network 75
2.26.1 Amplitude Excitation 75
2.26.2 Phase Excitation 77
2.26.3 Mutual Coupling 78
3.0 RESEARCH METHODOLOGY 80
3.1 Research Methodology Flowchart 80
3.2 Introduction to DGS Bandpass Filter 83
3.3 Proposal of a Parallel-Coupled DGS Bandpass Filter 84
3.3.1 Design Concept of the DGS Bandpass Filter 85
3.3.2 Design Methodology of the DGS Parallel-Coupled Bandpass Filter 89
3.4 Equivalent Circuit of the DGS Structure 92
3.5 Circuit Optimization in DGS Filter 97
3.6 The Simulated Circuit Layout of DGS Filter 98
3.7 The Fabricated Circuit Layout 99
3.8 Applying DR on Ground Plane of the DGS Filter 100
3.9 Preparation of Dielectric Material, Zirconate Tin Titanate ($ZrSnTiO_3$) 101
3.10 An Introduction to Multilayer Bandpass Filter 103
3.10.1 Proposal of a Multilayer Bandpass Filter 104
3.10.2 Design Methodology of Multilayer Bandpass Filter 105
3.10.3 Construction of Multilayer Bandpass Filter 106
3.11 The Simulated Circuit Layout of Multilayer Bandpass Filter 107
3.12 Modelling of the Multilayer Banpass Filter 109
3.13 The Fabricated Circuit Layout of the Multilayer Bandpass Filter 112

3.14 Proposal of a Simple Structure DR Bandpass Filter 116
3.14.1 Design Concept of the DR Filter 117
3.14.2 Design Considerations in Dielectric Resonator Filter 118
3.15 Simulated Circuit Layout of the DR Filter 119
3.16 Fabricated Circuit Layout of the DR Bandpass Filter 122
4.0 RESULTS AND DISCUSSION 123
4.1 Results from the DGS Parallel-Coupled Bandpass Filter 123
4.1.1 Comparison Result to other Researchers 127
4.1.2 Comparison of Circuit with and without DR 128
4.1.3 Results on Other Working Frequencies 131
4.2 Result from the Multilayer Bandpass Filter 135
4.2.1 Results from Gap Size Analysis 138
4.2.2 Radius Analysis of the Ring Resonator 140
4.3 Comparison Between the Multilayer and DGS Filters 141
4.4 Results from the Dielectric Resonator Filter 143
4.4.1 Analysis to Position DR on Transmission Line 146
4.4.2 Analysis to Position the DR Across the Transmission Line 154
4.4.3 Analysis on the DR Height, *h* 157
4.4.4 Analysis on Width of the Transmission Line 159
4.4.5 Analysis on the Conductor Thickness, *t* 160
4.4.6 Analysis on the Radius of the DR, *r* 162
4.4.7 Analysis on the Number of DRs 164
4.5 Comparison Between DGS and Dielectric Resonator Bandpass Filters 165
5.0 CONCLUSIONS AND FUTURE RECOMMENDATIONS 169
5.1 Overall Conclusion 169
5.2 DGS Parallel-Coupled Bandpass Filter 170
5.3 Multilayer Structure Bandpass Filter 170

5.4 Dielectric Resonator Bandpass Filter 171
5.5 Contribution of the Research 172
5.5.1 Contribution of DGS Parallel-Coupled Bandpass Filter 173
5.5.2 Contribution of Multilayer Structure Bandpass Filter 174
5.5.3 Contribution of DR Bandpass Filter 174
5.6 Future Works and Recommendations 175
REFERENCES 177
LIST OF PUBLICATIONS 185
APPENDIX 188

List of Figures

Figure 2.1: Signal passing through a parallel-coupled transmission line (Sen-Kuei *et al.*, 2010). 12

Figure 2.2: EBG structure from a periodic ground plane etching (a) Circuit configuration and (b) Responses (Radisic *et al.*, 1998a)..... 14

Figure 2.3: UC- EBG element (Yang *et al.*, 1999). 15

Figure 2.4 Schematic and results (a) Compact parallel-coupled BPF on the UC-EBG substrate and (b) Comparison Results (Yang *et al.*, 1999). 17

Figure 2.5: Two layer of EBG structure (Caloz *et al.*, 2001)..... 18

Figure 2.6: The view of DGS unit section (Kim *et al.*, 2000). 19

Figure 2.7: Schematic of proposed multi-pole bandpass filter (Zhu and Wu, 2002). 20

Figure 2.8: Microstrip EBG cells (a) EBG cell 1 and (b) EBG cell 2 (Xue *et al.*, 2000). 22

Figure 2.9: Simulated and measured S-parameters of the proposed EBG transmission line using the cell shown in Figure 2.8 (b) (Xue *et al.*, 2000). 23

Figure 2.10: Equivalent circuit for a single unit cell of the microstrip EBG structure (Collin, 1966). 25

Figure 2.11: Schematic of various shapes on the ground plane: (a) Folded slot with T-shape metal loading, (b) Folded slot (c) Corrugated slot and (d) rectangular slot (Zhang and Mansour, 2004). 27

Figure 2.12: Simulated S-parameters of the metal loaded slots (a) W = 2.8448 mm (b) W = 1.9304 mm (c) W=3.4036 mm and (d) W = 6.096 mm (Zhang and Mansour, 2004). 28

Figure 2.13: Schematic of a corrugated slot etched on the ground plane (Zhang and Mansour, 2004). 28

Figure 2.14: Simulated results for different length L and width W of the corrugated slots (Zhang and Mansour, 2004)..... 29

Figure 2.15: Schematic diagram of a folded slot with T-shaped metal loading etched on the ground plane (Zhang and Mansour, 2004). 30

Figure 2.16: Simulated S-parameters of the folded slot resonator (Zhang and Mansour, 2004). 31

Figure 2.17: Transmission line circuit model of the folded slot resonator (Zhang, 2007). 32

Figure 2.18: Comparison of the S-parameters of the folded slot resonator between transmission line model and EM simulation (Zhang, 2007). 35

Figure 2.19: RLC lumped-element circuit model of the folded slot resonator (Park *et al.*, 1999). 36

Figure 2.20: A comparison of the S-parameters from the RLC lumped-element and the EM simulation models (Chang *et al.*, 2001). 37

Figure 2.21: Schematic diagram of resonators with folded slots etched on the ground plane: (a) An interdigital capacitor and (b) A parallel-coupled line capacitor (Zhang, 2007). 38

Figure 2.22: Lumped-element circuit model of the resonator (Zhang, 2007)..... 38

Figure 2.23: Schematics of 2-pole microstrip bandpass filters (a) Interdigital capacitor and (b) Parallel-coupled line capacitor (Zhang, 2007). 39

Figure 2.24: TE_{01} multi-pole DR filter for cellular base-station applications (Fiedziuszko *et al.*, 2002). 41

Figure 2.25: Configuration of a TM mode DR filter (Kobayashi and Minegishi, 1988). 42

Figure 2.26: Dual-mode DR filter configuration (Fiedziuszko, 1982). 43

Figure 2.27: Quadruple-mode DR filter configuration (Hattori *et al.*, 2003). 44

Figure 2.28: Typical HE_{11} mode field distributions of the conductor-loaded resonator (Chi *et al.*, 1997a)..... 45

Figure 2.29: Configuration of the eight-pole conductor-loaded cavity filter (Chi *et al.*, 1997b). 46

Figure 2.30: Conductor-loaded dual-mode DR filter configuration (Hunter *et al.*, 1999). 47

Figure 2.31: Type of filters (a) Lowpass, (b) Highpass, (c) Bandpass and (d) Bandstop (Hong and Lancaster, 2001). 48

Figure 2.32: S-parameter relationships (Awang, 2006). 50

Figure 2.33: The cross section of a pair coupled microstrip lines (Young and Jones, 1980). 57

Figure 2.34: The microstrip EBG structure with termination electric and magnetic walls (Zhang, 2007). 60

Figure 2.35: Side view of the microstrip EBG structure from Figure 2.34 (Safavi-Naini and Macphie, 1982). 60

Figure 2.36: Cross-section view in the *x*-*y* plane of the N-furcated rectangular waveguide junction (Mansour and Macphie, 1985). 61

Figure 2.37: The cylindrical DR on a ground plane (Petosa, 2007). 71

Figure 2.38: Microstrip line (a) side coupling and (b) direct coupling (Petosa, 2007). 73

Figure 2.39: Power splitter junctions. 76

Figure 2.40: Passive phase delays a) Series and b) Parallel networks. 77

Figure 2.41: Mutual coupling (a) E-plane coupling and (b) H-plane coupling. 79

Figure 3.1 The methodology flowchart. 81

Figure 3.2: A parallel plate capacitor with a uniform dielectric inserted between the plates 86

Figure 3.3: Two parallel metal strips, each of width *w* and separated by a distance *h* 87

Figure 3.4: The proposed circuit layout (a) Top view and (b) Bottom view. 89

Figure 3.5: Equivalent circuit of the DGS. 92

Figure 3.6: Schematic circuit from ADS 96

Figure 3.7: Standing wave signal 97

Figure 3.8: The circuit layout from CST. 98

Figure 3.9: The fabricated circuit. 99

Figure 3.10: The circuit with DR (a) Top layer and (b) Bottom layer. 100

Figure 3.11: Fabrication process of the $ZrSnTiO_3$ ceramics. 102

Figure 3.12: $ZnSnTiO_3$ powder pressing procedures 103

Figure 3.13: Construction of the multilayer bandpass filter. 107

Figure 3.14: Dimensions of end-coupled resonator on the top layer. 108

Figure 3.15: Dimensions of split ring resonators in the inner layer. 108

Figure 3.16: Construction of the half split ring resonator and the equivalent circuit. 110

Figure 3.17: The fabricated circuit layout of the bandpass filter. 113

Figure 3.18: The overall equivalent circuit layout of the bandpass filter. 115

Figure 3.19: Schematic circuit simulated in ADS software 116

Figure 3.20: Geometry of the simulated bandpass filter. 119

Figure 3.21: Layout of dielectric resonators on the transmission line. 120

Figure 3.22: Geometry of the fabricated DR bandpass filter. 122

Figure 4.1: A comparison between simulated and measured results 124

Figure 4.2: Simulated results of modelling circuit 126

Figure 4.3: Comparison of the circuit after remove one wavelength optimization . 127

Figure 4.4: Measurement results of circuit with and without DR 129

Figure 4.5: A comparison of measurement results between the circuit with and without DR. 130

Figure 4.6: A comparison of measurement results between the circuit with and without DR for different band. 132

Figure 4.7: A comparison of measurement results between applying more than one DR. 133

Figure 4.8: DGS filter for X-band application 135

Figure 4.9: Comparison of S_{11} and S_{21} from simulation and measurement results. 136

Figure 4.10: Simulated results of modelling circuit from ADS simulator 138

Figure 4.11: Transformation of S_{11} when the gap size from the inner layer was varied. 139

Figure 4.12: Transformation of S_{21} when the gap size from the inner layer was varied. 139

Figure 4.13: Transformation of S_{11} when the length of split ring radius was varied. 140

Figure 4.14: Transformation of S_{21} when the length of split ring radius was varied. 141

Figure 4.15: Comparison of DGS and multilayer bandpass filters 142

Figure 4.16: Measured and simulated results of DR bandpass filter. 144

Figure 4.17: The effect of return loss when DR1 is moved along the transmission line. 149

Figure 4.18: The effect of insertion loss when DR1 is moved along the transmission line. 150

Figure 4.19: The effect of return loss when DR2 is moved along the transmission line. 151

Figure 4.20: The effect of insertion loss when DR2 is moved along the transmission line. 152

Figure 4.21: The effect of return loss when DR3 is moved along the transmission line. 153

Figure 4.22: The effect of insertion loss when DR3 is moved along the transmission line. 153

Figure 4.23: The effect of return loss when DR1 is moved across the transmission line. 154

Figure 4.24: The effect of insertion loss when DR1 is moved across the transmission line. 155

Figure 4.25: The effect of return loss when DR2 is moved across the transmission line. 155

Figure 4.26: The effect of insertion loss when DR2 is moved across the transmission line. 156

Figure 4.27: The effect of return loss when DR3 is moved across the transmission line. 156

Figure 4.28: The effect of insertion loss when DR3 is moved across the transmission line. 157

Figure 4.29: The effect of dielectric height on return loss. 158

Figure 4.30: The effect of dielectric height on insertion loss. 158

Figure 4.31: The effect of transmission line width, w on return loss, S_{11} when conductor thickness, t, is fixed at 0.035 mm. 159

Figure 4.32: The effect of transmission line width, w on insertion loss, S_{21}, when conductor thickness, t, is fixed at 0.035 mm. 160

Figure 4.33: The effect of conductor thickness, t, on return loss, S_{11}, when w is fixed at 2.18 mm. 161

Figure 4.34: The effect of the conductor thickness, *t*, on insertion loss, S_{21}, when *w* is fixed at 2.18 mm. 162

Figure 4.35: The effect of dielectric radius on insertion loss. 163

Figure 4.36: The effect of dielectric radius on return loss. 163

Figure 4.37: The effect of the number of DR on return loss. 164

Figure 4.38: The effect of the number of DR on insertion loss. 165

Figure 4.39: A comparison between DGS and the DR bandpass filters. 166

Figure 4.40: A comparison between the wideband DGS and the DR bandpass filters. 167

List of Tables

Table 2.1: Comparison between PBG and DGS(Weng *et al.*, 2008). 12

Table 3.1: Component values 95

Table 3.2: List of component values 115

Table 4.1: Critical points from measured and simulated results. 124

Table 4.2 Comparison results 128

Table 4.3: Critical points from the results of Figure 4.5 131

Table 4.4: Critical points from the results of Figure 5.4 133

Table 4.5: Critical points from the results of Figure 4.7 134

Table 4.6: Comparison of measured and simulated results. 137

Table 4.7: Critical points from the Figure 4.15 143

Table 4.8: Comparison values of simulation and measurement. 145

Table 4.9: Critical points from Figure 4.39. 166

Table 4.10: Critical points from Figure 4.40. 168

List of Abbreviations

1-D	One-dimensional
3D	Three Dimensions
BNC	Bayonet Neill-Concelman
BPF	Band Pass Filter
CAD	Computer Aided Design
CPU	Central Processing Unit
CPW	Coplanar Waveguide
CSRR	Complementary Split Ring Resonator
CST	Computer Simulation Technology
dB	Decibel
DE	Differential Equation
DGS	Defected Ground Structure
DR	Dielectric Resonator
EBG	Electromagnetic Band Gap
E-field	Electric Field
EM	Electromagnetic
FDTF	Finite Difference Time Domain
FEM	Finite Element Method
FR-4	Flame Retardant 4
GHz	Giga Hertz
HFSS	High Frequency Simulator Software
IE	Integral Equation
IEEE	Institute of Electrical and Electronics Engineers
IF	Intermediate Frequency

MHz	Mega Hertz
MIC	Microwave Integrated Circuit
MoM	Method of Moments
MTT-S	International Microwave Symposium
MWS	Microwave Studio
PBG	Photonic Band Gap
PCMFs	Parallel Coupled Microstrip Filters
PCML	Parallel-Coupled Microstrip Line
Q-factor	Quality factor
RF	Radio Frequency
S-parameters	Scattering parameters
SRR	Split ring resonator
SWR	Standing Wave Ratio
TE	Transverse Electric
TEM	Transverse Electromagnetic
TLM	Transmission Line Modeling
TM	Transverse Magnetic
UC	Uniplanar compact
W-CDMA	Wideband Code Division Multiple Access
WiMAX	Worldwide Interoperability for Microwave Access

List of Symbols

χ	Coupling amount
Φ	Phase angle
β	Propagation constant
ω	Angular frequency
γ	Complex propagation constant
α	Real part of propagation constant
π	Constant value (3.142)
ε	Dielectric constant
ϕ	Azimuth angle
ε_{eff}	Effective dielectric constant
Δf	Absolute bandwidth
λ_g	Guided wavelength
ω_o	Angle of resonant frequency
ε_r	Relative dielectric permittivity
λ_{sg}	Slot guided wavelength
$\overline{\boldsymbol{B}}$	Shunt normalized susceptance
∂	Angle loss
a	Dimension of component
A, B, C, D	Matrix elements
BW	Impedance bandwidth
c	Speed of light (3.0 × 108 m/s)
C	Capacitor
d	Periodicity

dc	Direct current
$E_{x(h)}$	Electric field of EBG slot
f_h	Upper cutoff frequency
f_l	Lower cutoff frequency
g	Gap
h	Height or thickness
H	Magnetic field
I	current
I_n	Incident and reflected TEM current amplitude
J_s	Electric source
L	Inductor
l	length
L_c	Length of coupling section
M_s	Magnetic source
N	Transformer turn ratio
n_{th}	Number of cascaded periodic structure
P_A *and* P_B	Diagonal matrices
P_{in}	Input power
P_o	Output power
R	Resistance
r	Radius
S	Spacing
S/*m*	Siemens per meter
S_{11}	Return loss
S_{21}	Insertion loss

T	Hermitian Transpose
$tan\ \delta$	Loss tangent
V	Volume
$V(h)$	Voltage across EBG slot with h substrate thickness
V_n	Incident and reflected TEM voltage amplitude
V_o	Output voltage
v_p	Phase velocity
W	Width
x	x-axis
y	y-axis
z	z-axis
Z_L	Load impedance
Z_M	Series impedance
Z_o	Characteristic impedance of transmission line
Z_p	Shunt impedance
Z_s	Slot impedance
Z_{sc}	Slot characteristic impedance
ε''	Dielectric loss
λ_o	Free space wavelength
Ω	Ohm

PEMBANGUNAN PENAPIS LALUAN JALUR GELOMBANG MIKRO MENGGUNAKAN STRUKTUR BUMI CACAT DALAM PERBANDINGAN DENGAN PENAPIS PELBAGAI LAPISAN DAN PENYALUN DIELEKTRIK

ABSTRAK

Penapis laluan jalur berfungsi melaksanakan tugas penting penapisan dalam sesebuah pemancar-terima radio. Jalur halangan yang sempit dan kecerunan rendah dalam kedua-dua jalur peralihan pada litar gandingan selari konvensional atau elektromagnet celahan jalur (EBG) merupakan dua (2) cabaran di dalam mereka bentuk penapis laluan jalur. Tesis ini akan memperkenalkan tiga (3) struktur penapis laluan jalur. Pertama adalah satu kombinasi baru gandingan selari dan struktur bumi cacat (DGS) beroperasi pada frekuensi pusat 7.8 GHz bagi kegunaan satelit mudah alih. Pada dasarnya, struktur gabungan ini telah menghasilkan faktor kualiti-Q yang tinggi dan gelombang peralihan yang menyumbang kepada cerun yang tinggi dan mengurangkan nilai tidak tetap (palsu). Penyalun dielektrik berbentuk silinder juga digunakan di dalam litar ini untuk meningkatkan kehilangan balikan dalam jalur laluan atau untuk meningkatkan kelebaran jalur. Penyalun dielektrik, Zirconate Tin Titanate, ZrSnTiO3 (ε_r = 37.4, kehilangan tangen = 0.002) dan bahan asas RO3003 dengan kehilangan pemalar dielektrik dan tangen masing-masing sebanyak 3.0 dan 0.0013, telah digunakan dalam projek ini. Keseluruhan Dimensi litar adalah 47.2 mm × 19.16 mm, manakala saiz DGS berbentuk segi empat tepat adalah 1 mm × 7.36 mm. Struktur kedua merupakan gabungan gandingan-hujung dan penyalun berbentuk cincin terpisah dalam struktur pelbagai lapis beroperasi pada frekuensi 3.47 – 3.79 GHz untuk applikasi *Worldwide Interoperability for Mocrowave Access* (WiMAX). Satu bentuk cincin terpisah yang diubah suai telah diperkenalkan untuk mendapatkan pertambahan beberapa sub-penyalun gandingan magnet di antara lapisan menegak bagi meningkatkan kesan gandingan tambahan dari struktur pelbagai lapis. Bahan

asas *Flame Retardant 4* (FR-4) dengan pemalar dielectrik, ε_r sebanyak 4.6 telah digunakan sebagai bahan utama. Struktur yang ketiga ialah gabungan litar penghantaran mudah bersama tiga (3) penyalun dielektrik berbentuk silinder berdasarkan konsep padanan rangkaian sukuan panjang gelombang untuk kegunaan jalur-X. Simulasi ketiga-tiga (3) struktur penapis ini menggunakan perisian gelombang mikro *Computer Simulation Technology* (CST), manakala pengukuran parameter-S menggunakan *Network Analyzer E8364B*. Keputusan simulasi menunjukkan penapis DGS telah memberikan nilai kehilangan masukkan minimum dan lebar jalur masing-masing sebanyak -0.62 dB dan 440 MHz pada jalur laluan. Struktur ini telah digunakan untuk mereka bentuk beberapa penapis bagi aplikasi yang lain untuk dibandingkan dengan penapis pelbagai lapisan dan penyalun dielektrik. Struktur pelbagai lapis mempunyai kehilangan masukkan minimum dan lebar jalur masing-masing sebanyak -2.86 dB dan 320 MHz. Berikutnya, penapis jalur lebar penyalun dielektrik mempunyai kehilangan memasukkan sebanyak -0.86 dB dan lebar jalur 1.28 GHz. Kajian menunjukkan bahawa apabila panjang talian penghantaran diubah, peralihan frekuensi berlaku. Kelebihan penapis DGS gandingan selari termasuklah: jalur peralihan yang sempit, keupayaan menawarkan kelebaran jalur yang luas, konfigurasi litar mudah, dan mudah untuk difabrikasi. Ia terbukti berdasarkan nilai-nilai ukuran dari semua litar mempunyai persamaan rapat dengan keputusan simulasi. Antara ketiga-tiga struktur, penapis gandingan selari DGS menunjukkan jalur peralihan terkecil dan jalur halangan yang luas.

DEVELOPMENT OF MICROWAVE BANDPASS FILTER USING DEFECTED GROUND STRUCTURE IN COMPARISON WITH MULTILAYER AND DIELECTRIC RESONATOR FILTERS

ABSTRACT

Bandpass filters perform an important filtering task in a radio transceiver. The narrow stopbands and low gradient in transition bands of conventional parallel-coupled or electromagnetic band gap (EBG) are two (2) of the challenges in designing a bandpass filter. This thesis will introduce three (3) structures of bandpass filter. The first is a new combination of parallel-coupled and defected ground structure (DGS) that operates at a center frequency of 7.8 GHz for mobile satellite application. In essence, this combination structure has resulted to high Q-factor and slow wave which contributes to a high slope and spurious suppression. Cylindrical dielectric resonators were also applied to the circuit in order to increase the return loss in the passband or to enhance the bandwidth of the design. The Zirconate Tin Titanate, $ZrSnTiO_3$ (ε_r = 37.4, tangent loss = 0.002) dielectric resonator and RO3003 substrate with dielectric constant and tangent loss of 3.0 and 0.0013 respectively were applied in this project. The overall dimension of the circuit was 47.2 mm × 19.16 mm, while the size of the rectangular DGS was 1 mm × 7.36 mm. The second structure is a combination of end-coupled and split ring resonators in a multilayer configuration that operate at 3.47 - 3.79 GHz for Worldwide Interoperability for Microwave Access (WiMAX) application. A modified split ring was introduced to obtain the additional sub-resonators from the magnetic coupled between vertical layers in order to increase the coupling effect from the multilayer structure. The Flame Retardant 4 (FR-4) substrate with dielectric constant, ε_r of 4.6 was used as a core material. The third structure is a combination of a simple transmission line and three (3) cylindrical dielectric resonators based on quarter wavelength matching network for X-Band application. Simulations of the three (3) filter structures were carried out using Computer Simulation Technology

(CST) Microwave Studio software while measurement of the S-parameters was analyzed using the E8364B Network Analyzer. Simulation results demonstrate the DGS filter has minimum passband insertion loss and bandwidth of -0.62 dB and 440 MHz, respectively. This structure was used to design a couple of filters for different applications in order to compare with the multilayer and dielectric resonator filters. The multilayer structure has a minimum insertion loss and a bandwidth of -2.86 dB and 320 MHz, respectively. Subsequently, the broadband dielectric resonator filter has minimum insertion loss of -0.86 dB and a bandwidth of 1.28 GHz. Investigations show that when the length of the transmission lines is varied, frequency shifting occurs. The advantages of the parallel-coupled DGS filter include: narrow transition bands, the ability to offer a broad bandwidth, simple circuit configuration, and finally, ease of fabrication. It was proven that the measurement values from all circuits are closely agreed to the simulation results. Among the three (3) structures, parallel-coupled DGS filter shows the smallest transition bands and wide stopbands.

CHAPTER ONE

1.0 INTRODUCTION

1.1 Background and Motivation

The advance of telecommunication systems in the modern world today increases the need of more sophisticated devices in supporting the variety of the applications. Ideally, a low loss filter passes a selected band of frequencies but attenuates frequencies out of the desired passband. The filter together with compact structures is required as a lot of applications are integrated in a single device. The filters with high quality rejection together with a broadband capacity will perform well in transmission data such as moving videos as well as high quality of audio. Good filters can reconfigure a communication system to facilitate an efficient utilization of the available frequency spectrum since there are demands in front-end receivers to suppress signal interferences.

A microstrip line incorporation with Defected Ground Structure (DGS) has been proven to exhibit good passband and stopband filter characteristics due to a slow wave effect (Kakhki and Neshati, 2010). These features have been used in bandstop filter applications to eliminate unwanted frequencies as well as to miniaturize microstrip filters. However, the filter skirt performance at both low and high frequency ends in conventional DGS are very low.

Previously, an improved stopband performance can be achieved only at the expense of the passband performance and vice versa (Crute and Davis, 2000). However, a good filter is needed to solve both the passband and the stopband

simultaneously. To achieve better performance, a combination of several approaches and structures such as parallel-coupled microstrip together with a rectangular DGS slot etched on the ground plane for a miniature microstrip bandpass filter which is one of the alternatives that can be further investigated (Boutejdar *et al.*, 2008a).

Multilayer design structures offer more advantages in certain areas as compared to single layer structures (Brzezina *et al.*, 2007; Zhang *et al.*, 2011). These advantages include the size reduction of the transmission line due to the freedom of dielectric materials selection while it is also flexible in layout since a transmission line can be arranged on different layers. It is able to contribute to a higher coupling effect due to the transmission lines being arranged in dual-direction; vertically and horizontally. However, some of the materials could not be simply attached together. Hence, the selection of substrate materials in a multilayer structure is one of the challenges that need to be considered if the circuit is going to be fabricated.

Most of the works reported in the literature have focused on tunable bandpass filters through insertion loss which are determined by the quality factor (Q). Due to the superior characteristic of high Q and miniaturization and the dielectric resonator (DR), filters are preferred in designing a microwave circuit. The demands on high quality filters are increased especially on low loss and compact tablet of DR which is capable of being manufactured in a large quantity at a reasonable low cost (Novgorodov *et al.*, 2009).

Future wireless technologies need a solution to replace the low Q-factor of microstrip and coaxial filters by a new approach of using low cost DR filters that

offer higher value of Q. This thesis will also describe the realization of the DR bandpass filter with the combination of simple microstrip lines.

1.2 Problem Statement

A microwave bandpass filter with a compact size, high quality in terms of performance together with a low cost is a necessity. A parallel-coupled bandpass filter has advantages in term of ease of synthesis (Scott, 1993), low cost, and high realizable of manufacturing (Young and Jones, 1980). However, a low order filter can only contribute to a compact size but could not solve the problem of wide transition bands. Cascading the filters will reduce the problem in the bands but would simultaneously increase the overall circuit size and high level of harmonic in stopband after the cutoff frequency. Incorporation microstrip lines with DGS on a ground plane has been proven to exhibit wide stopband filtering characteristics which result from a slow wave effect. However, the sharp cut-off between the passband and stopband characteristics in the conventional parallel-coupled or DGS remain unsolved and therefore, need to be investigated in order to obtain a better performance (Tahanian *et al.*, 2010).

Basically, the amount of coupling in end-coupled filter is very low (Bin and Uysal, 1998). However, this can be increased by the presence of a long overlapped region between any other resonators (Pal, 2006). Conventionally, doing this will cause a drawback of increasing the overall circuit size with a large value of capacitance being obtained from the structure (Bin and Uysal, 1998).

A lot of efforts were put into deep investigations on various innovative designs of the ring resonator structure due to the advantage of open-ended angle of 360° (Yu-Zhen *et al.*, 2008; Woo-Chul *et al.*, 1999) even when the typical bandwidth of the resonator is less than 5% (Chul-Soo *et al.*, 2005). The structure of the ring resonator can be modified in order to obtain a compact size which will increase the coupling effect by introducing gaps into the shape. Since the overall perimeter of the ring is controlled by the radius, it becomes a new challenge to obtain a high coupling effect and a compact circuit simultaneously,

A tight couple between the resonators can be very complicated to be realized from a fabricated circuit (Pozar, 1990). A multilayer structure is able to overcome that restriction (Lee S-J, 2004; Jia-Sheng and Lancaster, 1999). The structure was proposed to reduce the size of microwave devices (Courreges *et al.*, 2010; Bairavasubramanian and Papapolymerou, 2007) where a well known method of realizing the miniature filters is by fabricating the multilayer structures on a high dielectric substrate (Jia-Sheng and Lancaster, 1999). In this context, a filter is constructed from a combination of inductors and capacitors. It must be noted that the contradiction features between both the components could not be resolved by simply selecting a high dielectric constant material because in order to obtain high value of capacitances and inductances simultaneously, the substrates must be chosen from a different type of dielectric constants or thicknesses.

Dielectric resonator (DR) is widely used to enhance the performance of microwave communication devices such as filters and resonators as provides a low design profile and wide bandwidth (Petosa, 2007). A variety of geometrical

resonators such as rectangular, circular and rings have been reported (Virdee and Trinogga, 1988). The combination of DR and strip line has derived substantial research interests due to their ease in circuit realization for both series and shunt, and it requires no via holes (Young and Jones, 1980; Edwards, 1992; Street *et al.*, 1997). The addition of DR on strip line was introduced in antenna in order to obtain high return loss in passband (Ain *et al.*, 2008). However, the DR on microstrip line is still open for further investigation especially in obtaining a wideband using the array approach.

1.3 Objectives

Generally a bandpass filter is designed to allow certain frequencies called passband while rejecting others. Therefore, a wide stopband and a sharp cutoff response are important in designing a bandpass filter. The main objective of this project is to design new structures of bandpass filter that can be fabricated and measured for confirmation. In achieving this, several methods proposed by other researchers were reviewed and investigated. An in-depth investigation on the effect of material thickness using the electromagnetic simulation software was carried out. All the objectives of this project can be summarized as follows:

1) To design a parallel-coupled DGS bandpass filter for a high magnetic coupling. The same structure is used to design a few frequency bands for comparison. The design must be unique and its can contribute to small transition bands.

2) To develop a multilayer bandpass filter with a unique structure in order to obtain a high electromagnetic coupling from both vertical and horizontal directions. The circuit will be fabricated and measured to confirm for the desired aim. The results from this filter were compared to DGS design in order to identify the optimum design structure.
3) To identify through investigation, a new simple structure of dielectric bandpass filter using few tablets of high dielectric permittivity to improve the bandwidth of the circuit. Some parameters including the dielectric size and the distance to locate the tablets will be investigated using an electromagnetic simulator in order to obtain the optimum response. This circuit was intensively used to investigate the dielectric effect on the filter due to the simple structure and it shows a clear relationship between DR and microstrip line.

1.4 Scope of Works

The overall project will focus on three different structures of bandpass filter. The first is a combination of parallel-coupled and DGS, the second is the combination of a modified split ring and end-coupled in a multilayer structure and the third is the dielectric resonator bandpass filter based on quarter wavelength matching approach.

The first structure is a combination of a parallel-coupled microstrip transmission lines together with a rectangular DGS etched on the ground plane for the miniature of the filter. A unique open circuit stub is introduced to both input and

output ports to ensure the impedance matching. The design covers simulation, measurement and comparison between both results in order to confirm the design objectives. Apart from that, a few other working frequencies were also designed, fabricated and measured to prove that the new structure can operate at any application. A study on introducing DR into the circuit was also carried out to improve the filter performance.

The second design is a new modified split ring resonator that has not been explored by other researchers hitherto. The ring resonator's shape consists of several folded transmission lines, creating few additional sub-resonators vertically from the end-coupled resonator on the top layer. This structure allows the magnetic field to cross polarize along the ring axis. Then, the induced current loops pass through the distributed capacitance along the split-ring perimeter in the middle layer. The performance of this filter was then compared to the DGS structure. Several parameters such as gap size and radius of the ring that influence the filter response were investigated in order to gain the relationship of the filter response.

The third structure is a design of a bandpass filter using few high permittivity ceramic tablets on a transmission line which involves the impedance matching between the microstrip and DRs. The design consists of three dielectric resonators in an array topology. The purpose of the array dielectric resonators is to generate additional frequencies that can be merged together to produce a wideband device. Study on the placement of the first, second and third dielectric resonators were done in order to identify the location for optimum impedance matching.

All designs were calculated and simulated with the help of CST Microwave Studio, while the measurement of the S-parameters done using the E8364B Network Analyzer.

1.5 Thesis Organization

Following Chapter 1, Chapter 2 provides an intensive literature review of various latest planar microstrip filters with DGS including slot configurations which have been studied by previous researchers. A series of filters introduced by the researchers will be taken into consideration in order to highlight the advantages and disadvantages of the designs before taking some of the approaches to build up several new structures. This chapter will ensure that the design of this project will not be involve the same designs that have been explored by the other researchers. The novelty of the design will become one of the most important criteria in this research. It includes the theory of filters, quarter wavelength, air gap and the most important elements such as capacitors and inductors. Other factors such as the benefit of dielectric resonators including the coupling and mutual effect in obtaining a good filter response will also be explained.

Chapter 3 is a detail explanation on the project that encompasses the design methodology and circuit modelling. The explanations started from the main circuit which is a new structure of parallel-coupled DGS, followed by the multilayer and lastly a dielectric resonator. There are circuit layouts from simulation software together with detail dimensions as well as the fabricated devices that are used in testing and measuring.

In Chapter 4, results from the three proposal structures throughout the period of the study were presented to relate the theory of electronics and microwave respectively. The width, length and strip line thickness influence the responses of the filter were investigated and analyzed to present signal transformation patterns and their relationships. Comparisons between the filter responses were also carried out in order to show the advantages and disadvantages of each design.

Lastly, a summary of contributions including the advantages from all designs were highlighted in Chapter 5. There were still rooms for further exploration in some of the investigations before more conclusions could be derived. The expected areas for future investigation were suggested in order to provide more opportunities for future researchers.

CHAPTER TWO

2.0 LITERATURE REVIEW

2.1 Introduction

Microstrip transmission line together with various perforation approaches on the ground plane has attracted attention due to their amenability to standard fabrication processes of microwave integrated circuit (MIC). Several method attempts to control the effectiveness of electromagnetic wave propagation through DGSs have been described in the literature (Rui *et al.*, 2001; Yongxi and Itoh, 1999) that include various shapes and sizes. Structures such as Uniplanar Compact Electromagnetic Bandgap (UC-EBG) (Yang *et al.*, 1999; Woonphil and Bomson, 2002) and DGSs have been successfully applied in the microstrip construction of microwave devices such as filters and antennas (Ahn *et al.*, 2001; Park *et al.*, 2002).

Microstrip together with Electromagnetic Bandgap (EBG) structures on ground plane in a filter exhibits an acceptable passband and wide stopband simultaneously due to slow-wave characteristic in the circuit (Yongxi and Itoh, 1999; Rumsey *et al.*, 1998). These features can be used in bandpass, bandstop or lowpass filter applications to eliminate unwanted frequencies as well as to reduce the physical size of microstrip circuits. The concept and application of microstrip EBG structures have been reported (Hu *et al.*, 2000; Karmakar *et al.*, 2002; Lee *et al.*, 2002). Despite offering various advantages and wide applications gain from the microstrip EBG structures, there are still problems in utilizing such structures.

2.2 Review on the Concept of Aperture Slot

An aperture slot is also known as a Defected Ground Structure (DGS) if the slot is realized by etching a defect on ground plane of planar circuits. This defect disturbs the shield current distribution in the ground plane and changes the characteristics of transmission line such as line capacitances and inductances. Consequently, using one or a small number of unit cells, DGS is able to provide wide bandstop characteristic in certain frequency bands.

Photonic Band Gap (PBG) structure is a periodic structure which is very similar to DGS in modifying guided wave characteristics which exhibits a wide stopband property. Using a microstrip line as an example, a periodic structure will be etched in ground plane where the PBG will modify the properties of the microstrip line such as its characteristic impedance and propagation constant (Dahmardeh *et al.*, 2009).

DGS is very much motivated by a study of PBG to change guided wave properties where it makes one or few of the PBG etched on ground plane. The shape of the slot can also be modified from a simple hole to a more complicated shape. Table 2.1 compares the features between PBG and DGS where in PBG, the geometry is a periodic structure while in DGS, it normally contains one or few structures etched on the ground plane. However, both of the PBG and DGS are similar in terms of microwave properties such as propagation constant and characteristic impedance. The main difference between the two is in terms of the equivalent circuit extractions. There is a more complex equivalent circuit in PBG due to its periodic structures compared to the single DGS which depend on the number of the repeated shapes. If

the circuit involves the PBG, the analysis becomes more complicated due to the interaction of mutual couple between each slot (Weng *et al.*, 2008).

Table 2.1: Comparison between PBG and DGS(Weng *et al.*, 2008).

Features	**Photonic Band Gap Structure (PBG)**	**Defected Ground Structure (DGS)**
Geometry	Periodic etched structure	One or few etched structure
Microwave properties	Similar	Similar
Equivalent circuit exaction	Complex circuit	Simple RLC circuit

2.3 Basic Properties of DGS

The simplest DGS has only one perforated slot on ground plane. Figure 2.1 demonstrates a signal passing through a parallel-coupled transmission line from the source. When the DGS is applied in the middle of the microwave circuit, then E-field is discontinued along the middle line of coupler and acts as an open circuit for the even mode. Signal flows in even mode transmission line will pass through a series stub and will be slowed down by the DGS (Sen-Kuei *et al.*, 2010).

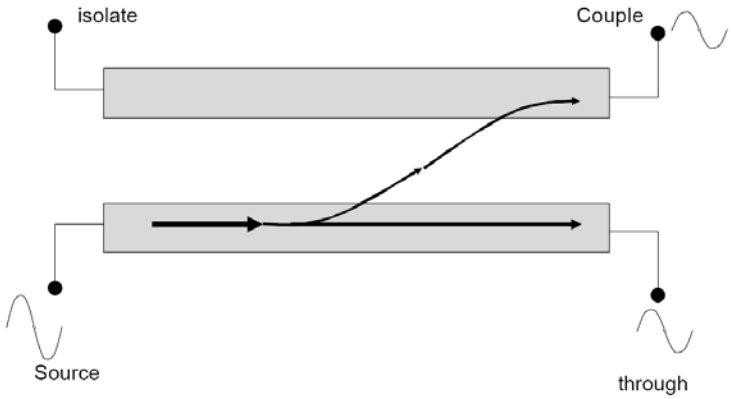

Figure 2.1: Signal passing through a parallel-coupled transmission line (Sen-Kuei *et al.*, 2010).

The relationship between the phase velocity and effective dielectric constant can be presented in Equation 2.1 where the effective dielectric constant, ε_{eff} is inversely proportional to the phase velocity, v_p since c is a constant value equal to the speed of light. From this equation, the DGS acts as a delay line to slow down the signal flows through the transmission line.

$$v_p = \frac{c}{\sqrt{\varepsilon_{eff}}} \Rightarrow \varepsilon_{eff} = \left(\frac{c}{v_p} \right)^2 \tag{2.1}$$

This concept of delay line is applicable only when the transmission line is in even mode. This means that when the signal passing through the circuit in an even mode the phase velocity of the wave will be decreased due to the ε_{eff} being increased from the above relationship. For example, in a device with three DGS using the concept of delay line, the delay of signal in the even mode with three DGS is longer than the circuit with only one DGS. So the implication from the concept of the delay line on the ε_{eff} can be enhanced if the number of DGS increases, hence the coupling coefficient will be subsequently improved. In other words, the DGS can control the coupling coefficient by modifying the transmission line properties. However, in an odd mode the signal does not slow down due to the phase velocity and where ε_{eff} are independent to the DGS (El-Hang, 2010; Mu *et al.*, 1985).

2.4 Electromagnetic Band Gap (EBG)

This is relatively similar to the aperture slot but with a periodic structure either on the substrate or on the ground plane. Implementing EBG structures by etching a number of periodic patterns on the ground plane as shown in Figure 2.2 contribute to

several advantages such as low cost and easy in fabrication process as compared to multilayer structures (Radisic *et al.*, 1998a). Apart from that, they are compatible with the standard planar circuit technology for microwave applications.

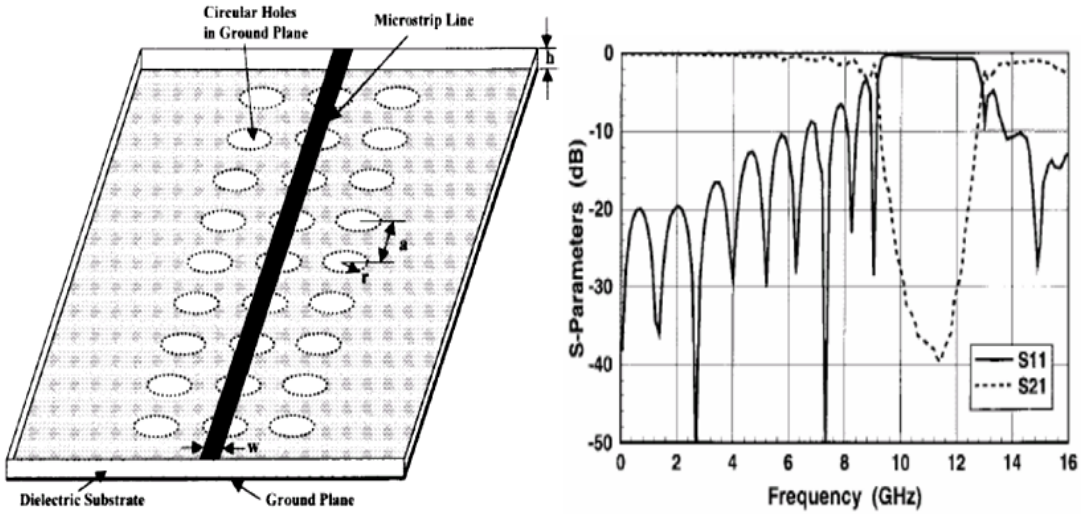

(a) (b)

Figure 2.2: EBG structure from a periodic ground plane etching (a) Circuit configuration and (b) Responses (Radisic *et al.*, 1998a).

Several variations of microstrip transmission lines incorporating EBG structures provide an effective method to reject unwanted frequencies and to reduce the physical size of the microstrip circuits (Hu *et al.*, 2000; Lee *et al.*, 2002; Karmakar *et al.*, 2002). Mostly the circuits consisted of two-dimensional periodic holes etched on the ground plane. The EBG shapes vary from simple rectangular or circular shapes to more complicated profiles while the arrangement of the EBG holes vary from square or triangle lattices to others. The shape and size of the lattices have a considerable impact on the passband and stopband characteristics (Bao and Ammann, 2007).

2.5 Uniplanar-Compact EBG Structures

The development and upgrading of compact EBG such as the Uniplanar–Compact (UC)-EBG structures (Yang *et al.*, 1999) that consist of a two-dimensional square pattern; metal pad and four connecting narrow branches to form a distributed *LC* network is illustrated in Figure 2.3. This structure is able to introduce a slow wave effect generated by the unique shape (Yang *et al.*, 1999). The size of periodicity in the EBG lattice is only $0.1\lambda_o$ at the stopband frequency and hence can be considered as a compact structure. This structure can be build by implementing a standard planar fabrication technique without any modifications. The virtues of low loss and uniplanar features make the UC-EBG structure a very promising candidate as a slow-wave transmission line.

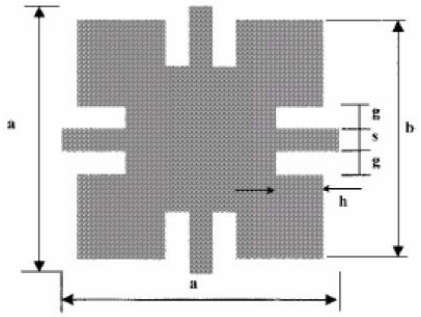

Figure 2.3: UC- EBG element (Yang *et al.*, 1999).

The slow-wave transmission line is able to reduce the spurious content in conventional microstrip filters where high level of spurious in passband will deteriorate the performance of the overall RF system. In normal circumstances, extra cascaded or higher filter orders are required to suppress the spurious modes but this approach will cause a draw back to the increment of insertion loss in the passband as well as increasing the size of the overall circuit. Compact microstrip filters with

intrinsic spurious rejection can be constructed by employing the UC-EBG structure that has been introduced as shown in Figure 2.3. With this structure, the device is able to derive a wide and deep stopband concurrently that suppresses the spurious in passband especially the high level of harmonics. Furthermore, extra filters are not required as the stopband is an intrinsic feature of the device. The slow-wave feature is also able to reduce the physical length of the filter, consequently reducing the overall circuit area.

Figure 2.4 (a) shows the schematic of a compact parallel-coupled microstrip filter on a top side and UC-EBG structure on the ground plane. The measured results of the compact parallel coupled bandpass filter on the UC-EBG are shown in Figure 2.4 (b) together with a conventional microstrip bandpass filter for comparison. This clearly shows that the isolations of the conventional filter are -10 dB and -5 dB at 12 GHz and 17 GHz, respectively. It must be noted here that the filter on the UC-EBG ground exhibits a 30-40 dB suppression of the spurious transmissions (Yang *et al.*, 1999).

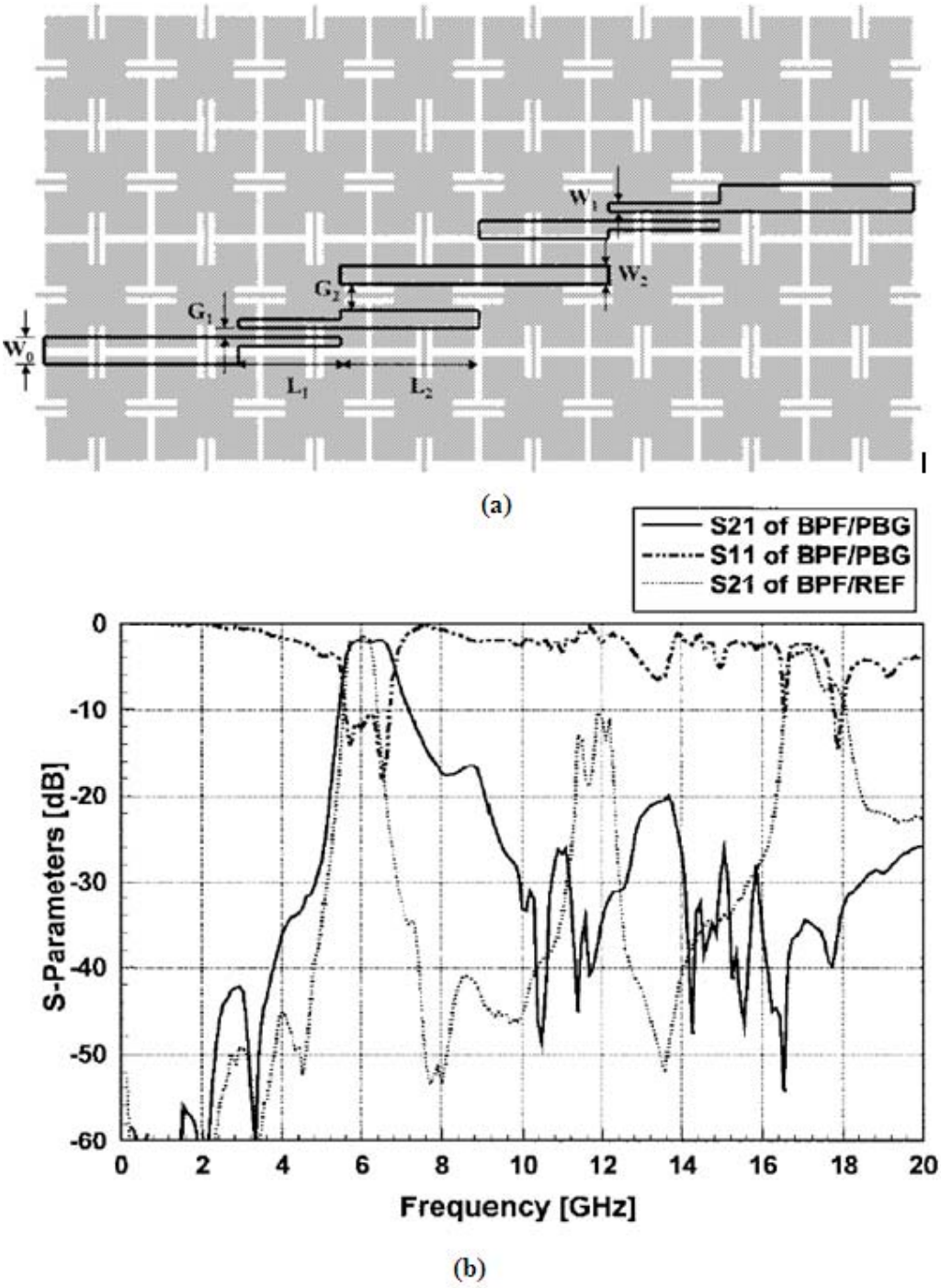

Figure 2.4 Schematic and results (a) Compact parallel-coupled BPF on the UC-EBG substrate and (b) Comparison Results (Yang *et al.*, 1999).

2.6 Multilayer EBG Structures

A good example of a multilayer EBG structure is a uniplanar compact electromagnetic bandgap (UC-EBG) (Caloz *et al.*, 2001). The EBG patterns are etched on two different ground plane substrates with height, h_1 and h_2 of a single layer uniplanar circuit and stacked. This structure is claimed to be able to derive much wider stopbands than those of the single layer UC-EBG. Figure 2.5 shows the two layers bi-periodic microstrip structure of a stacked UC-EBG plates with different periodicities (Caloz *et al.*, 2001). The two layers structure configuration with an effective periodicity of 2*a*, leading to the realization of a compact EBG structure which means that the EBG from both layers will only repeat the same alignment simultaneously for every 2*a*.

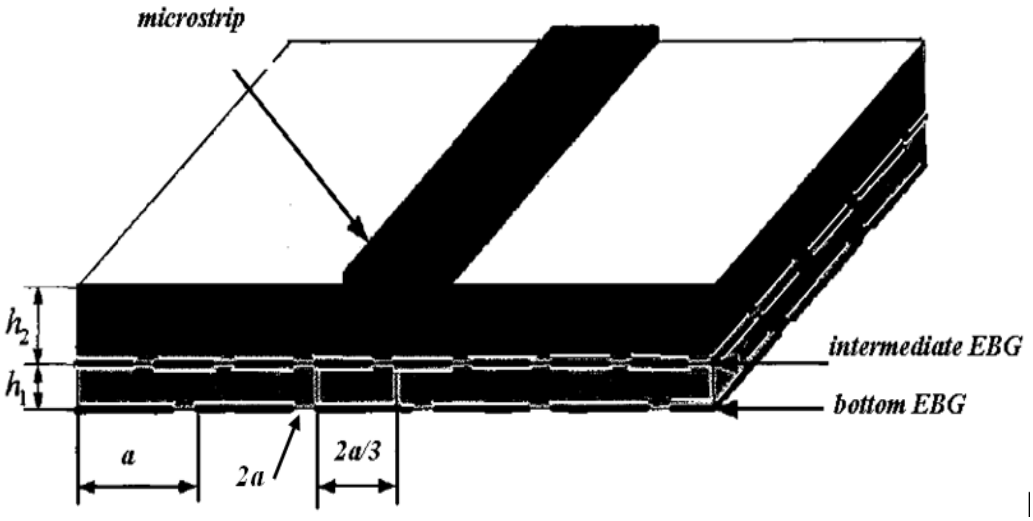

Figure 2.5: Two layer of EBG structure (Caloz *et al.*, 2001).

2.7 Defected Ground Structure (DGS)

DGS is a simple method that provides high rejection band. The DGS series will group either the periodic patterns known as EBG or non-periodic patterns which are able to offer a wide rejection band due to the increment of the effective inductance of a transmission line. These advantages have been employed in many circuits such as planar antennas, filters, power amplifiers and power dividers (Ahn *et al.*, 2001; Park *et al.*, 1999; Radisic *et al.*, 1998b). DGS integrated with a microstrip line shown in Figure 2.6 was claimed to have superior stopband quality (Kim *et al.*, 2000).

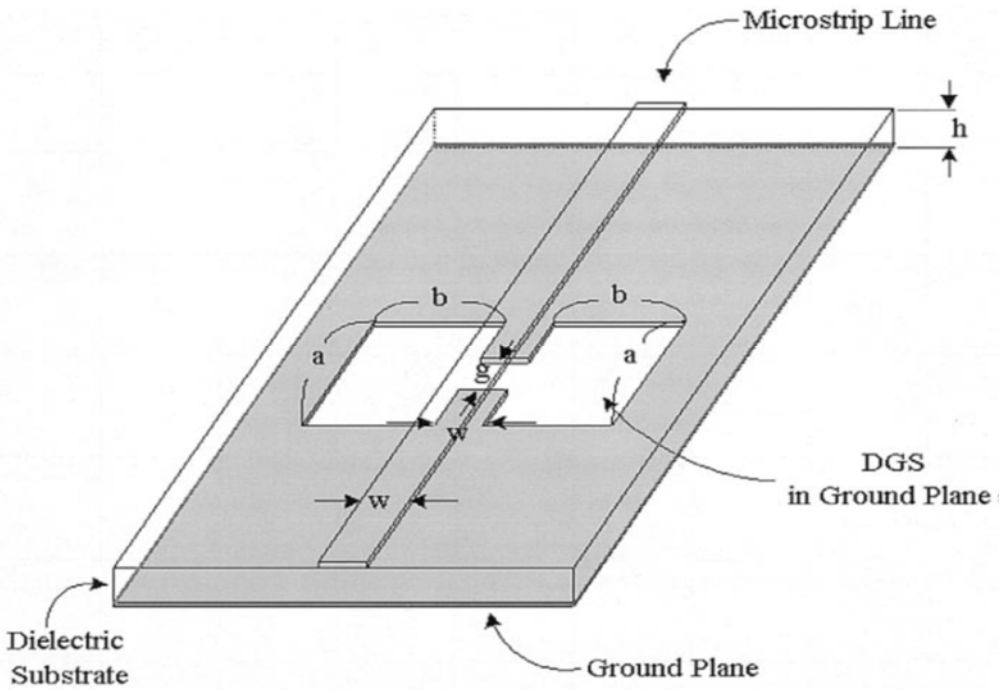

Figure 2.6: The view of DGS unit section (Kim *et al.*, 2000).

The changing in the shape size of the DGS includes narrow and wide etched areas on the metallic ground plane which have the capability of increasing the effective capacitance and inductance in a transmission line. The example of applying this structure in designing a lowpass filter is able to produce high impedance

inductance with a relatively large conductor width which consequently helps to improve the power handling capability of the lowpass filter (Ahn *et al.*, 2001).

Another example of DGS was applied in multi-pole bandpass filter shown in Figure 2.7. The researchers exploited a DGS by etching rectangular apertures on the ground plane of a parallel-coupled microstrip line (PCML) for the effective enhancement of a tight frequency dependent coupling (Zhu and Wu, 2002). This concept has been proven where it was applied in the designing of a compact wideband microstrip bandpass filter.

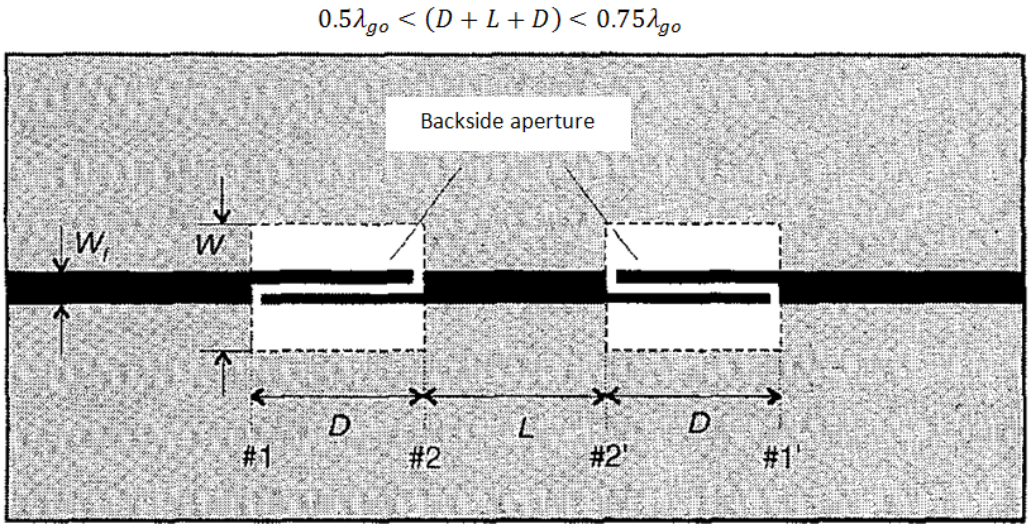

Figure 2.7: Schematic of proposed multi-pole bandpass filter (Zhu and Wu, 2002).

2.8 Perforation in Transmission Lines

In conventional EBG, the microstrip line must be carefully oriented on a substrate. However, in the perforated transmission lines, the dependence of the location and orientation of the microstrip line on the propagation constant is

completely eliminated. Where this is concerned, the perforated transmission line structures have a lot of potential applications in microstrip circuits such as filters, antennas and amplifiers (Boutejdar *et al.*, 2008a).

According to the transmission line theory (Awang, 2006), the propagation constant of a lossless line is

$$\beta = \omega_o\sqrt{LC} \tag{2.2}$$

where ω_o is the angular frequency, while L and C are the distributed series inductance and shunt capacitance per unit length respectively. A slow-wave can be achieved if a large β is obtained from high values of L and C due to the wave velocity is inversely proportional to the propagation constant such as shown in the relationship below (Nghiem and Williams, 1990);

$$v_p = \frac{\omega_o}{\beta} = \frac{1}{\sqrt{LC}} \tag{2.3}$$

Consequently, it is possible to form an EBG structure on the transmission line if the values of L and C are increased periodically and not continuously (Xue *et al.*, 2000). In Figure 2.8, two cells containing of one-dimensional (1-D) was proposed where the cells of microstrip line with some metals have been removed. By comparing the EBG cell 1 and cell 2 from Figure 2.8(a) and (b), , the two narrow lines act as series inductance in Figure 2.8(a) become one line in Figure 2.8(b). These narrow lines are able to increase the value of the series inductance. On the other hand, the gaps across the width of transmission line result in the increment of the shunt capacitance.

Cascading these cells as an EBG on a microstrip line will present a slow-wave that produces a superior stopband in a filter such as other EBG with ground perforations. With the width of gaps and lines of the perforation maintaining the same, the cell in Figure 2.8(b) provides a more effective slow-wave and bandgap than that obtained from Figure 2.8(a). Figure 2.9 shows the simulated and measured S-parameters from the EBG transmission lines using combination of six EBG cells from Figure 2.8 (b).

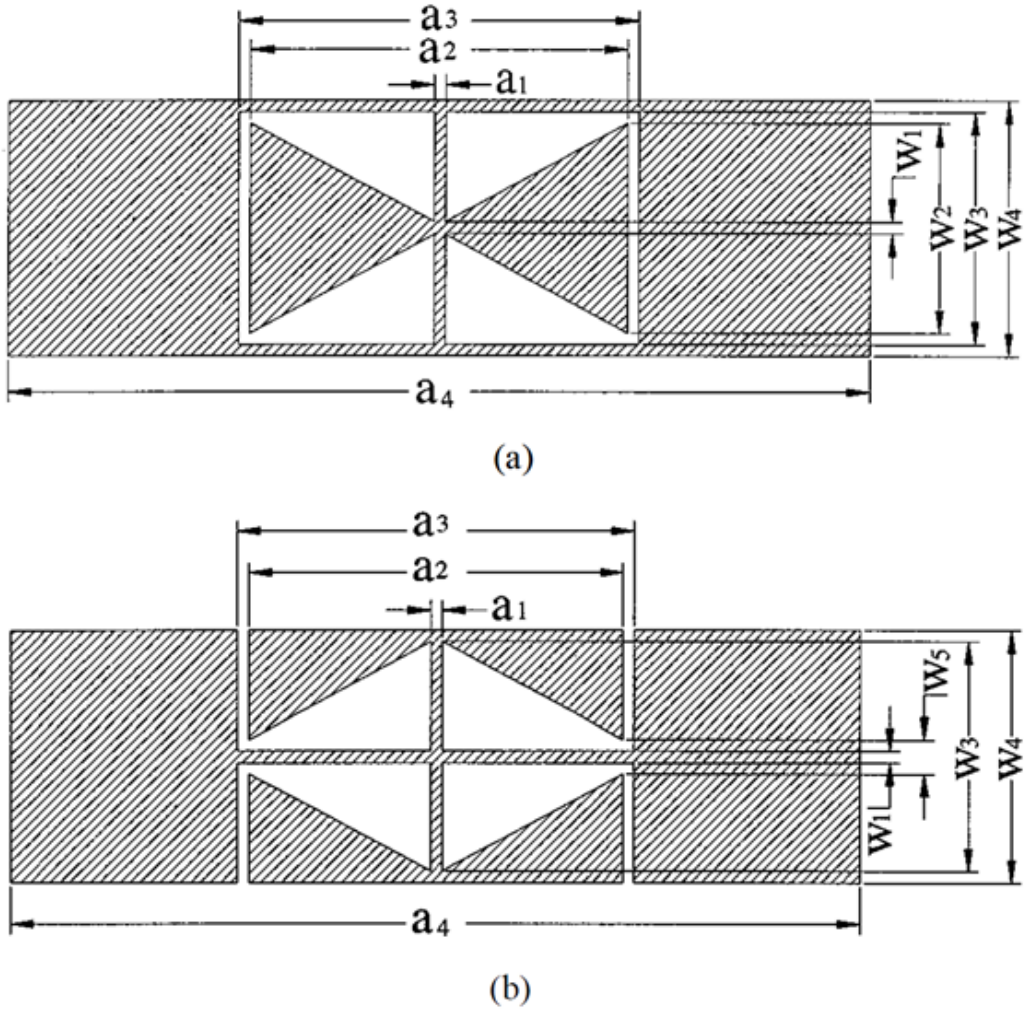

Figure 2.8: Microstrip EBG cells (a) EBG cell 1 and (b) EBG cell 2 (Xue *et al.*, 2000).

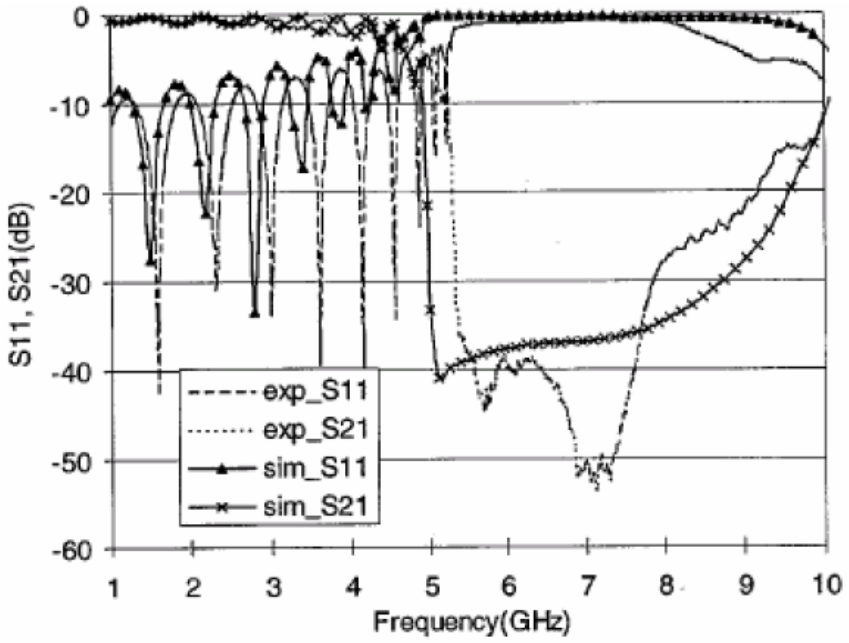

Figure 2.9: Simulated and measured S-parameters of the proposed EBG transmission line using the cell shown in Figure 2.8 (b) (Xue *et al.*, 2000).

2.9 Problems of Conventional Microstrip EBG Structures

In ideal filter situations, losses caused by conductor or dielectric substrate are ignored. However in reality, when an electromagnetic wave propagates through a periodic structure, there are certain frequency bands separated between passband and stopband. The band that allow wave to propagate is known as passband which is separated by two cutoff frequencies. In practical, there will be another band called transition band which exists due to the imperfection of material or due to the existence of material loss.

The performance of a microstrip EBG is derived according to the bandwidth of the passband, stopband, the rejection level and the insertion loss ripples in the passband. In order to obtain a high performance from a microstrip EBG; small transition bands, a deep rejection level and small passband ripples are necessary. However, in the conventional microstrip EBG, there will always be a conflict between the stopband and the passband characteristics (Yang *et al.*, 1999; Radisic *et al.*, 1998a).

Previous researchers found that varying the size of the etched hole or the number of holes produces better insertion loss in passband and a better stopband rejection at the expense of the passband. In this context, reducing the size of the hole improves the return loss but degrades the stopband characteristics. In order to achieve the optimum performance, a tradeoff is required between the number and size of the etched holes (Yang *et al.*, 1999).

A simple one dimensional transmission line periodic structure analysis demonstrates the problem that has been carried out (Collin, 1966). An equivalent network of a single unit cell is a shunt normalized susceptance $\bar{B}$ with transmission lines length, $l = d/2$, where d represents the periodicity of the structure on both sides as depicted in Figure 2.10. The values of V_n and I_n represent the total amount of incident and reflected Transverse Electromagnetic (TEM) voltage and current amplitudes, respectively. The figure shows a relationship of voltage and current at the input and output of the n_{th} section in the cascaded periodic structure.

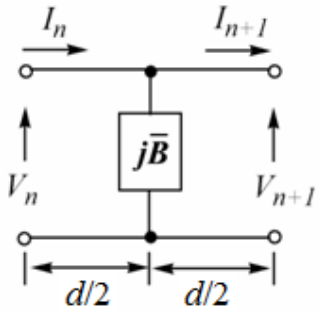

Figure 2.10: Equivalent circuit for a single unit cell of the microstrip EBG structure (Collin, 1966).

Characteristics of a periodic structure in transmission line can be evaluated by determining the complex propagation constant $\gamma = \alpha + j\beta$ for the overall size of the circuit area. The propagation constant can be obtained by solving the following characteristic equations (Collin, 1966).

$$\begin{bmatrix} A & B \\ C & D \end{bmatrix} - \begin{bmatrix} e^{\gamma d} & 0 \\ 0 & e^{\gamma d} \end{bmatrix} \begin{bmatrix} V_{n+1} \\ I_{n+1} \end{bmatrix} = 0 \tag{2.4}$$

where A, B, C and D are the elements of the ABCD matrix of the unit section from Figure 2.10. For the initial condition, the equation of determinant circuit without input and output voltage as well as current is zero;

$$\begin{vmatrix} A - e^{\gamma d} & B \\ C & D - e^{\gamma d} \end{vmatrix} = AD - BC + e^{2\gamma d} - e^{\gamma d}(A + D) = 0 \tag{2.5}$$

If the periodic structure is supporting a propagation wave, the voltage and current at the $(n = 1)_{th}$ terminal should be exactly the same as the voltage and current at the n_{th} terminal which is a phase delay due to finite propagation time.